Institute of Physics Publishing Journal of Physics: Conference Series **54** (2006) 22–28
doi:10.1088/1742-6596/54/1/004 Galaxy Center Workshop 2006

Shock interactions between Sgr A East and its environments

Sungho Lee[1], Soojong Pak[2], T. R. Geballe[3], Sang-Gak Lee[4], Christopher J. Davis[5], Minho Choi[1], Y. C. Minh[1,6], Robeson M. Herrnstein[7] and Paul T. P. Ho[8,9]

[1]Korea Astronomy and Space Science Institute, 61-1 Hwaam-dong, Yuseong-gu, Daejeon 305-348, South Korea
[2]Department of Astronomy and Space Science, Kyung Hee University, Yongin-si, Gyeonggi-do 446-701, South Korea
[3]Gemini Observatory, 670 N. A'ohoku Place, Hilo, HI 96720, USA
[4]Astronomy Department, School of Physics and Astronomy, Seoul National University, Shillim-dong, Seoul 151-742, South Korea
[5]Joint Astronomy Centre, University Park, 660 North A'ohoku Place, Hilo, HI 96720, USA
[7]Department of Astronomy, Columbia University, 550 West 120th St. New York, NY 10027, USA
[8]Academia Sinica Institute of Astronomy and Astrophysics, P.O. Box 23-141, Taipei, 106 Taiwan
[9]Harvard-Smithsonian Center for Astrophysics, 60 Garden Street, Cambridge, MA 02138, USA

E-mail: `leesh@kasi.re.kr`

Abstract. We have surveyed the interaction regions between Sgr A East and the surrounding molecular clouds in the H_2 $1-0$ S(1) (2.1218 μm) line emission. The resulting data cube shows the distribution of the H_2 emission both in space (with a resolution of about 2 arcsec) and in velocity (with a resolution of about 18 km s^{-1}). Our data are compared with NH_3(3,3) data from radio observations to investigate the gas kinematics. Based on the H_2 $1-0$ S(1) line's intensity, its ratio to H_2 $2-1$ S(1), and its gas kinematics, we conclude that the emitting H_2 is excited by strong molecular shocks. We estimate shock velocities ($\simeq$ 100 km s^{-1}) by comparing the H_2 line profiles with those of NH_3, and derive an initial explosion energy of $0.2 - 4 \times 10^{53}$ ergs. Such a high energy excludes a single normal supernova for the origin of Sgr A East. We examine other hypotheses, including the tidal disruption of a star by the supermassive black hole (Sgr A*), multiple supernovae, and a hypernova. We suggest that a hypernova, which is believed to originate from a collapsar or microquasar, is the most probable origin.

1. Introduction

Sgr A East is believed to play an essential role in the large-scale structure and kinematics of the central 10 pc of our Galaxy. However, the nature of Sgr A East is still controversial. The object frequently has been interpreted as a supernova remnant (SNR) because of its shell structure and non-thermal spectrum in the radio [1, 2]. Some recent studies, however, have suggested that the energy, size, and elongated morphology of Sgr A East cannot have been produced by a typical supernova [3, 4, 5]. A theoretical study [6] suggested that Sgr A East may be the

[6] Present address: Academia Sinica Institute of Astronomy and Astrophysics, P.O. Box 23-141, Taipei, Taiwan

remnant of a solar mass star tidally disrupted by a 10^6 $M_\odot$ supermassive black hole (SMBH), of which Sgr A* is the most probable candidate. This model can explain the elongated shape of Sgr A East as well as the extreme energetics ($\sim 4 \times 10^{52}$ ergs). However, observations by the *Chandra X-ray Observatory* [7] suggested that Sgr A East should be classified as a metal-rich 'mixed morphology' remnant of a single Type II supernova explosion with an energy of 10^{51} ergs. Another study using NH_3 data [8] estimated the energy of the progenitor explosion of Sgr A East as $2 - 9 \times 10^{51}$ ergs.

The energy required to make the Sgr A East shell is a key parameter to understanding its origin and can be directly measured by studying the interaction of the shell with the ambient material. Sgr A East is surrounded by various molecular structures including two giant molecular clouds (GMCs) M-0.02-0.07 and M-0.13-0.08 (also known as the '50 km s^{-1} cloud' and the '20 km s^{-1} cloud', respectively), and several filamentary molecular features: the 'molecular ridge', the 'southern streamer', the 'northern ridge', and the 'western streamer' (contours in Figure 1 and refer to [8, 9]). Previous studies of the interaction, however, are mostly based on indirect evidence from morphology, kinematics of neighboring molecular clouds, or absorption of background radiation, rather than on direct, physical interactions involving Sgr A East. To investigate the origin of Sgr A East, we have observed molecular hydrogen (H_2) line emission, which is an excellent tracer of interactions between energetic wind sources such as Sgr A East and dense molecular clouds.

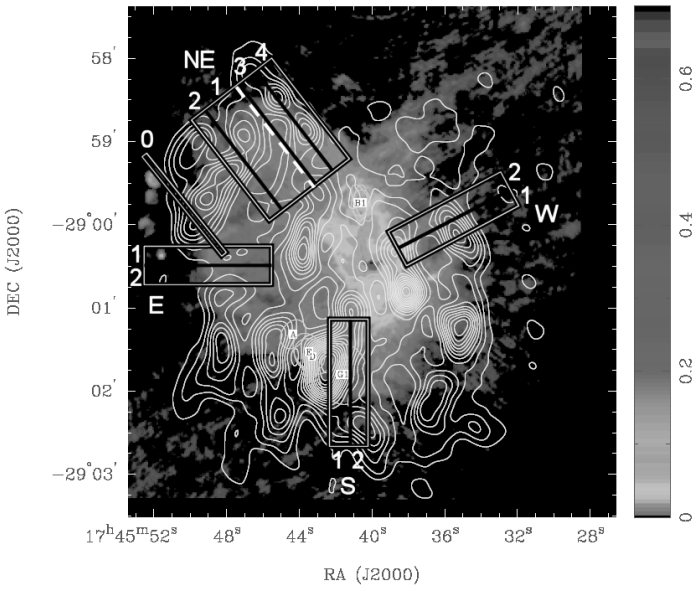

Figure 1. The background image is the 6 cm continuum map of the central 10 pc with $NH_3(3,3)$ emission contours superimposed [9]. Sgr A East surrounds Sgr A* and Sgr A West in the radio continuum. The four fields observed in H_2 1–0 S(1) are indicated by the labelled white boxes. Each field is divided into 2 or 4 scanning blocks labelled with numbers. The narrow box labelled '0' belongs to field E. The white dashed line in field NE-1 indicates the slit position of the H_2 2−1 S(1) observation. Contour levels are in intervals of 4 σ, where σ = 0.33 Jy beam^{-1} km s^{-1} (with the $\sim$ 15" × 13" beam), and the scale bar ranges from 0 to 0.7 Jy beam^{-1} (where the beam size is 3.4" × 3.0").

2. Observations and data reduction

Four fields around Sgr A East were observed in H_2 1−0 S(1) with a slit-scanning technique (see Figure 1). The H_2 2−1 S(1) line (2.2477μm) also was observed at the location where the H_2 1–0 S(1) emission is brightest. The data were obtained at the 3.8 m United Kingdom Infrared Telescope (UKIRT) during 2001 and 2003 using the Cooled Grating Spectrometer 4 [10] with its 31 l/mm echelle, 300 mm focal length camera, and two-pixel-wide slit. The pixel scale along the slit was 0.90 arcsec for H_2 1−0 S(1) and 0.84 arcsec for H_2 2−1 S(1); the slit widths on the sky were 0.83 and 0.89 arcsec, respectively, for these two configurations. The angular resolution was about 2 arcsec ($\sim$ 0.1 pc at the distance to the Galactic centre [11]) and the spectral resolution

was ~ 18 km s^{-1} for both lines. The slit length was ~ 90 arcsec, which allowed a large area to be efficiently surveyed.

After the data were flatfielded through the UKIRT reduction pipeline ORAC-DR, we employed standard IRAF[1] routines to perform sky subtraction, interpolate over bad pixels, remove image distortions, and impose an accurate (to ± 1 km s^{-1}) wavelength calibration using telluric OH lines. We also removed stellar continua and residual skylines, and flux-calibrated using the spectra of HR 6496 and HR 6310.

The final stage of data reduction involved the use of MIRIAD [12, 13], a program package generally used for reduction and analysis of radio interferometric data. However, MIRIAD can also be used for the general reduction of continuum and spectral line data such as our near-infrared H_2 data. We employed MIRIAD to stack the 2-dimensional (2-D) spectral images into a single 3-dimensional (3-D) data cube for each of the fields and then combined them into a total data cube (Figure 2) that contains coordinate information for every position along every slit for each slit orientation [14].

3. H_2 excitation mechanism

The near-infrared H_2 emission arises either from thermal excitation by shocks or from non-thermal excitation by absorption of far-ultraviolet (far-UV) photons. The H_2 2–1 S(1) / 1–0 S(1) line ratio, which is the most commonly used indicator of excitation mechanism, can distinguish between UV in low-density ($n(H_2) < 5 \times 10^4$ cm^{-3} [15]) gas, UV in dense gas, jump-shocks (J-shocks) [16], slow J-shocks [17], and continuous-shocks (C-shocks) [17, 18].

From the observed line ratios of 0.3 – 0.5 [19], we can rule out many of the above possibilities, but cannot distinguish between fast J-shocks, a dense PDR, or by a combination of fluorescence and shocks. However, fast J-shocks are excluded since J-shocks typically produce lower H_2 $1-0$ S(1) line intensities ($< 10^{-4}$ ergs s^{-1} cm^{-2} sr^{-1} or $< 3 \times 10^{-18}$ W m^{-2} arcsec^{-2} [16]) than our observed results (5 – 20 $\times 10^{-18}$ W m^{-2} arcsec^{-2}).

We can also consider the kinematic information obtained from the observed line profiles. In a pure PDR or in a J-shock the H_2 line profiles are narrow. In a PDR the line is un-shifted with respect to the cloud velocity, whereas in a J-shock it is shifted by more than ~ 20 km s^{-1}. C-shock profiles are broad extending from the ambient cloud velocity to the shock velocity. To investigate the kinematic properties of both the excited (hot) gas and ambient (cool; < 100 K) gas, we compare the high resolution H_2 $1-0$ S(1) line profiles with the NH_3(3,3) line profiles [9], at eight representative positions where bright emission lines of both molecules are detected (see Figure 2).

For most spectra in Figure 3, the H_2 line widths are much larger (typically 50 – 100 km s^{-1}) than the NH_3 line widths (typically 20 – 40 km s^{-1}). Because of a blending of five hyperfine lines, the observed NH_3 line widths may be greatly overestimated and the recovered intrinsic line widths are about 15 km s^{-1} [20]. Thus we conclude that the H_2 lines are much broader than the NH_3 lines, by as much as 30 – 80 km s^{-1}, and exclude the pure fluorescence models. Fast J-shocks also seem to be inconsistent with our results, owing to the low peak velocities of the H_2 lines relative to the NH_3 lines. Instead, the gas kinematics indicates C-shocks. However, the high values (up to 0.5) of the line ratio at some positions [19] point to fluorescent contributions. Therefore, a combination of C-shocks and fluorescence [21] is the most reasonable explanation for the H_2 excitation.

[1] IRAF is distributed by the National Optical Astronomy Observatories, which are operated by the Association of Universities for Research in Astronomy, Inc., under cooperative agreement with the National Science Foundation.

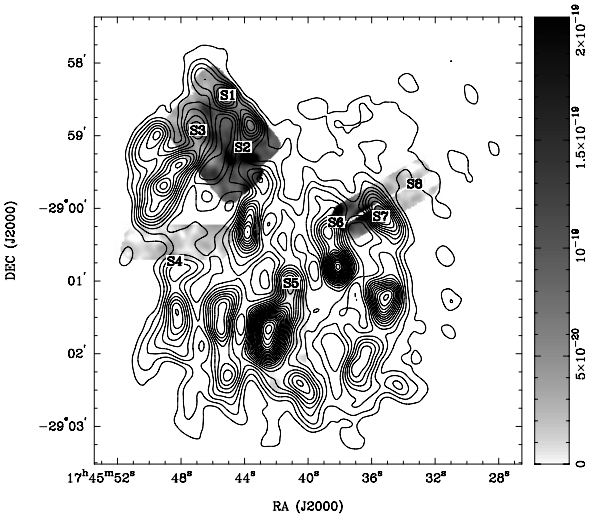

Figure 2. Integrated intensity map of H_2 $1-0$ S(1) line emission, smoothed by a Gaussian with FWHM = 5". The gray-scaled intensity level is indicated by the right hand bar in units of W m^{-2} arcsec^{-2}. The overlaid contours show the velocity-integrated NH_3(3,3) emission map [9]. The contour levels are in intervals of 3σ (the RMS noise $\sigma = 0.33$ Jy beam^{-1} km s^{-1}). The positions of the eight spectra of H_2 $1-0$ S(1) and NH_3(3,3) in Figure 3 are marked on the map.

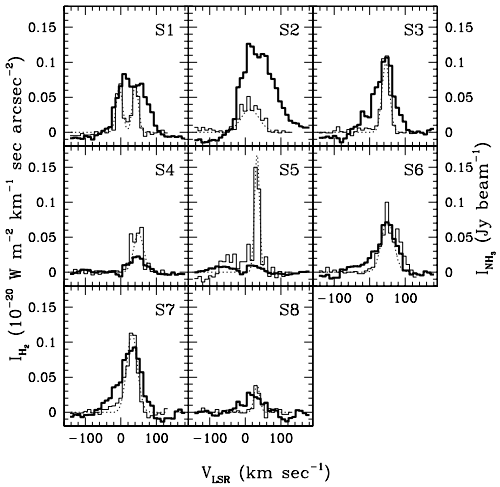

Figure 3. Spectra of H_2 $1-0$ S(1) and NH_3(3,3) in 30" FWHM apertures at the positions marked in Figure 2. Thick solid lines are the H_2 $1-0$ S(1) spectra, for which the intensity scale is indicated on the left-side, and thin solid lines NH_3(3,3), for which the scale is on the right-side. The dotted lines are Gaussian fits to the NH_3(3,3) line profiles. The spectra were obtained by convolving each data cube with a circular Gaussian beam and are not corrected for instrumental broadening in velocity.

4. Shock velocities of Sgr A East from line profiles

Since the radiation is emitted as the gas is being heated and accelerated in the shock front [22], the speed of a C-shock can be determined from the velocity corresponding to the edge of the line profile, hereafter denoted by V_{max}. According to detailed models for the line profiles of C-shocks [23], the full-width-at-zero-intensity (FWZI) of a line is 90 per cent of the shock velocity. Because line profiles from different regions are often superimposed, however, the low velocity edge (the pre-shock velocity) of an individual shock profile is not always obvious. Thus, instead of using the FWZI to determine the speed of the C-shock, we use the difference between V_{max,H_2} of a post-shock H_2 profile and V_{0,NH_3}, the system velocity of the pre-shock gas as traced by the NH_3 emission.

The velocity of NH_3 line center (V_{0,NH_3}) is measured from a Gaussian fit and V_{max,H_2} is determined from a deconvolved profile (using a Gaussian of FWHM = 18 km s^{-1} to approximate the instrumental resolution [14]). The resulting line-of-sight velocities of the C-shocks range from 44 km s^{-1} to 128 km s^{-1} depending on the location. After corrections for geometrical projection effects assuming an oblate shell for the Sgr A East shock front [14], the mean velocity of the shocks is 109 ± 34km s^{-1}. The detailed results are presented elsewhere [14].

The derived shock velocities seem to be too large to be acceptable in typical C-shock models, which have breakdown velocities of < 50 km s^{-1} [24]. The breakdown velocity, however, depends on the density and magnetic field strength in the pre-shock gas [25]. It is generally thought that a magnetic field of a few mG exists throughout the Galactic Center region [26]. In such a strong magnetic field and in clouds of mean density 10^4 cm^{-3} [27], the breakdown velocity is increased

to > 200 km s^{-1}.

5. Explosion energy and age of Sgr A East

To estimate the initial energy and the age of Sgr A East we use a standard model [28] of the evolution of a SNR in a medium of uniform density. Sgr A East is thought to be in a pressure-driven radiative phase (or snowplow phase) [4, 7, 8]. Then the energy of the initial explosion, E_0, is given by

$$E_0 = 4.3 \times 10^{51} \left(\frac{E_{shell}}{10^{51}\ \mathrm{ergs}}\right)^{2/3} \left(\frac{R_{shell}}{1\ \mathrm{pc}}\right)^{4/3} \left(\frac{n_0}{10^4\ \mathrm{cm}^{-3}}\right)^{2/3} \quad [\mathrm{ergs}]$$

$$E_{shell} = \frac{2\pi}{3}\ R_{shell}^3\ n_0\ m_H\ V_{shell}^2$$

where R_{shell} is the current radius of the shell, n_0 is the mean initial H number density of the pre-shock gas, m_H is the proton mass, and V_{shell} is the expansion velocity of the shell material [4], which is assumed to be the same as the mean velocity of the molecular shocks. For n_0 we suppose two extreme cases: a dense giant molecular cloud (scenario I), and a low density halo [7] (scenario II).

In scenario I, shocks with a mean velocity of $V_{shock} = 109$ km s^{-1} are propagating through molecular clouds with mean H_2 densities of $n_{H_2} = 10^4$ cm^{-3} [27]. Thus $V_{shell,I} = V_{shock} = 109$ km s^{-1} and $n_{0,I} = 2\ n_{H_2} = 2 \times 10^4$ cm^{-3}. Since the mean shell radius, $R_{shell} = 4.6$ pc, which is derived from the elliptical boundary of 5.4 pc $\times$ 3.8 pc [14], the shell's kinetic energy is calculated to be $E_{shell,I} = 2.3 \times 10^{52}$ ergs and the initial explosion energy $E_{0,I} = 4.2 \times 10^{53}$ ergs.

In scenario II, we assume that the shock front of Sgr A East has just started to contact its surrounding molecular clouds and the shocks are slowed down by dense gas. Since the measured shock velocities from the H_2 lines are for these slowed shocks, we use instead the velocities of fast shocks that propagated through the low density gas halo before contacting the molecular clouds. The velocity of the fast ambient shocks in the halo can be derived using $V_{s,halo}/V_{s,cloud} = \sqrt{n_{cloud}/n_{halo}}$ where $n_{halo} = 10^3$ cm^{-3} [7]. It is reasonable to regard the compressed shell as the synchrotron shell which contacts the inner edge of the dust ring [4]. Hence we use $R_{shell,II} = 3.7$ pc, which is smaller by 80 per cent than the size determined from the H_2 emission. Using $V_{s,cloud} = 109$ km s^{-1} and $n_{cloud} = 2 \times 10^4$ cm^{-3}, we calculate $V_{shell,II} = V_{s,halo} = 487$ km s^{-1} and $n_{0,II} = n_{halo} = 10^3$ cm^{-3}. Then the kinetic shell energy is calculated to be $E_{shell,II} = 1.2 \times 10^{52}$ ergs and the initial explosion energy $E_{0,II} = 2.7 \times 10^{52}$ ergs.

We can calculate the age of Sgr A East from

$$t = 114\ \left(\frac{R_{shell}}{0.329\ \mathrm{pc}}\right)^{7/2} \left(\frac{E_0}{10^{51}\ \mathrm{ergs}}\right)^{-3/4} \left(\frac{n_0}{10^4\ \mathrm{cm}^{-3}}\right) \quad [\mathrm{yr}],$$

using the estimated explosion energy, E_0 [28]. Then the estimated age is 2.5×10^4 yr in scenario I and 4.6×10^3 yr in scenario II.

6. Origin of Sgr A East

The explosion energy of 0.2 – 4 $\times 10^{53}$ ergs excludes the hypothesis of a single, typical supernova with a kinetic energy of 10^{51} ergs for the origin of Sgr A East.

The predicted frequency (once every 10^4–10^5 yr) of the tidal disruption of stars by a SMBH and energy released (0.4 – 4 $\times 10^{53}$ ergs) [6] are consistent with our estimates of the age and explosion energy, respectively. On the other hand, to explain the 3-D geometry of the Sgr A complex, this model needs a highly collimated eruption since Sgr A*, which is thought to be the source of explosion (i.e. the SMBH), is located at the edge of Sgr A East along the line of

sight [8, 14]. An anisotropic explosion, however, is not likely according to detailed studies of the evolution of stellar debris [29, 30]. In addition, this model cannot reproduce the high metallicity observed in X-ray [7] since the explosion is driven by gravity rather than by nuclear reactions.

The extremely large energy of the Sgr A East explosion may be explained by typical supernovae if several tens of them explode over a short time span, which cannot be longer than the age of Sgr A East ($\sim 10^4$ yr). This might be possible in a stellar cluster containing a huge number of massive stars, in which many stars have similar masses so that their SN-end-lifetimes have a very small dispersion. In the Galactic center, there are three extraordinarily massive and dense young clusters; the Central, Arches, and Quintuplet clusters. Using the estimated initial masses [31] and evolution models of massive stars [32, 33], we calculate the SN-end-lifetimes of the member stars in the Arches cluster as an example. Figure 4 shows that the estimated lifetimes are concentrated around 4500 kyr, which corresponds to $M_{init} \simeq 40$–70 $M_\odot$. The peak at that age contains $\sim$50 stars and covers $\sim 3 \times 10^5$ yr, corresponding to an average supernova rate of slightly more than one per 10^4 yr. Thus at most only a few explosions are expected during the lifetime of Sgr A East, and multiple supernovae cannot account for its energy.

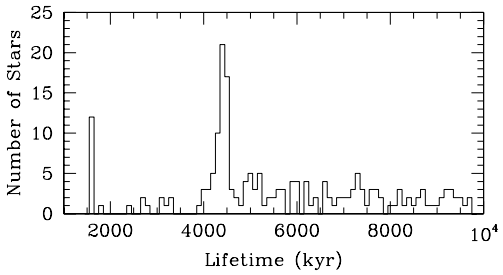

Figure 4. Histogram for the lifetimes of the stars in the Arches cluster. The data are binned by 10^5 yr for the lifetime.

The extremely high energies ($> 10^{52}$ ergs) of hypernova [34, 35] can be reproduced by black hole formation mechanisms such as a "collapsar" or "jet-powered supernova (JetSN)" [33, 36], or the "microquasar" model [34]. Either occurrence satisfies both the energy and metallicity constraints. There are many potential cadidate hypernovae near Sgr A East. JetSNe are possible in the range of $M_{init} \simeq 25$–60 $M_\odot$ (GRBs are also possible when $M_{init} > 35$ $M_\odot$) under the metallicity condition in the Galactic center [36]. In the Arches cluster, for example, there are $\sim$ 130 massive stars in the potential mass range of JetSNe and $\sim$ 80 stars in the range of JetSNe+GRBs. These numbers may be doubled if the Central and Quintuplet clusters, which have similar properties with the Arches cluster, are included. We conclude that only the hypothesis of a hypernova can satisfy all the observational constraints above.

7. Future work

The interstellar medium in the central 10 pc is known to be very clumpy and dense. Thus the evolution of Sgr A East needs to be studied using more realistic, numerical simulations than the standard analytic model. For the black hole origin, only the tidal disruption model has been tested in this work, but disruption is only one possibility related to SMBHs. Other phenomena observed in active galactic nuclei, e.g. bursts or outflows, should also be examined as possible origins of Sgr A East. Note also that a very inhomogeneous environment near the site of the explosion might circumvent the problem of high collimation. Finally, the viability of the hypernova model should be also examined based on its other properties; for example, its radio or X-ray emission.

Acknowledgments
We thank the staff at UKIRT for their excellent support during our observations. S. Lee thanks Luis Ho for the insightful suggestions on future work. Fig. 1 is reproduced from Fig. 10 of [9] by permission of the AAS. The United Kingdom Infrared Telescope is operated by the Joint Astronomy Centre on behalf of the U.K. Particle Physics and Astronomy Council. This work was financially supported by the BK21 Project of the Korean Government. T. R. Geballe's research is supported by the Gemini Observatory, which is operated by the Association of Universities for Research in Astronomy, Inc., on behalf of the international Gemini partnership of Argentina, Australia, Brazil, Canada, Chile, the United Kingdom and the United States of America.

References

[1] Jones T W 1974 *A&A* **30** 37
[2] Goss W M, Schwarz U J, Ekers R D and van Gorkom J H 1983 *Proc. IAU Symp.* vol 101 ed J Danziger and P Gorenstein (Dordrecht: Reidel) p 65
[3] Yusef-Zadeh F and Morris M 1987 *ApJ* **320** 545
[4] Mezger P G, Zylka R, Salter C J, Wink J E, Chini R, Kreysa E and Tuffs R 1989 *A&A* **209** 337
[5] Fatuzzo M, Melia F, Yusef-Zadeh F and Markoff S 1999 *ASP Conf. Ser.* vol 186 ed H Falcke et al (San Francisco: ASP) p 560
[6] Khokhlov A and Melia F 1996 *ApJ* **457** L61
[7] Maeda Y et al 2002 *ApJ* **570** 671
[8] Herrnstein R M and Ho P T P 2005 *ApJ* **620** 287
[9] McGary R S, Coil A L and Ho P T P 2001 *ApJ* **559** 326
[10] Mountain C M, Robertson D J, Lee T J and Wade R 1990 *Proc. SPIE* vol 1235 ed D L Crawford (Bellingham: SPIE) p 25
[11] Reid M J 1993 *ARA&A* **31** 345
[12] Sault R J, Teuben P J and Wright M C H 1995 *ASP Conf. Ser.* vol 77 ed R A Shaw et al (San Francisco: ASP) p 433
[13] Hoffman W, Hudson J, Sharpe R K, Grossman A W, Morgan J A and Teuben P J 1996 *ASP Conf. Ser.* vol 101 ed G H Jacoby and J Barnes (San Francisco: ASP) p 436
[14] Lee S 2005 *PhD thesis* Seoul National University
[15] Black J H and van Dishoeck E F 1987 *ApJ* **322** 412
[16] Hollenbach D and McKee C F 1989 *ApJ* **342** 306
[17] Smith M D 1995 *A&A* **296** 789
[18] Kaufman M J and Neufeld D A 1996 *ApJ* **456** 611
[19] Lee S, Pak S, Davis C J, Herrnstein R M, Geballe T R, Ho P T P and Wheeler J C 2003 *MNRAS* **341** 509
[20] McGary R S and Ho P T P 2002 *ApJ* **577** 757
[21] Fernandes A J L, Brand P W J L and Burton M G 1997 *MNRAS* **290** 216
[22] Hollenbach D J, Chernoff D F and McKee C F 1989 *Proc. of the 22nd Eslab Symp.* vol SP-290 ed B H Kaldeich (European Space Agency) p 245
[23] Smith M D and Brand P W J L 1990 *MNRAS* **243** 498
[24] Draine B T, Roberge W G and Dalgarno A 1983 *ApJ* **264** 485
[25] Smith M D, Brand P W J L and Moorhouse A 1991 *MNRAS* **248** 730
[26] Chuss D T, Davidson J A, Dotson J L, Dowell C D, Hildebrand R H, Novak G and Vaillancourt J E 2003 *ApJ* **599** 1116
[27] Güsten R and Philipp S D 2004 *Proc. of the 4th Cologne-Bonn-Zermatt Symp.* vol 91 ed S Pfalzner et al (Heidelberg: Springer) p 253
[28] Shull J M 1980 *ApJ* **237** 769
[29] Lee H M and Kim S S 1996 *JKAS* **29** 195
[30] Bogdanović T, Eracleous M, Mahadevan S, Sigurdsson S and Laguna P 2004 *ApJ* **610** 707
[31] Figer D F et al 2002 *ApJ* **581** 258
[32] Woosley S E, Langer N and Weaver T A 1993 *ApJ* **411** 823
[33] Woosley S E, Heger A and Weaver T A 2002 *Rev. Mod. Phys.* **74** 1015
[34] Paczyński B 1998 *ApJ* **494** L45
[35] Nakamura T, Umeda H, Iwamoto K, Nomoto K, Hashimoto M, Hix W R and Thielemann F-K 2001 *ApJ* **555** 880
[36] Heger A, Fryer C L, Woosley S E, Langer N and Hartmann D H 2003 *ApJ* **591** 288